ISMI: A classification index for High Angular Resolution Diffusion Imaging

D. Röttger‡, D. Dudai‡ D. Merhof* and S. Müller‡

‡ Institute for Computational Visualistics, University of Koblenz-Landau, Germany
* Visual Computing, University of Konstanz, Germany

ABSTRACT

Magnetic resonance diffusion imaging provides a unique insight into the white matter architecture of the brain in vivo. Applications include neurosurgical planning and fundamental neuroscience. Contrary to diffusion tensor imaging (DTI), high angular resolution diffusion imaging (HARDI) is able to characterize complex intra-voxel diffusion distributions and hence provides more accurate information about the true diffusion profile. Anisotropy indices aim to reduce the information of the diffusion probability function to a meaningful scalar representation that classifies the underlying diffusion and thereby the neuronal fiber configuration within a voxel. These indices can be used to answer clinical questions such as the integrity of certain neuronal pathways. Information about the underlying fiber distribution can be beneficial in tractography approaches, reconstructing neuronal pathways using local diffusion orientations. Therefore, an accurate classification of diffusion profiles is of great interest. However, the differentiation between multiple fiber orientations and isotropic diffusion is still a challenging task. In this work, we introduce ISMI, an index which successfully differentiates isotropic diffusion and single and multiple fiber populations. The classifier is based on the orientation distribution function (ODF) resulting from Q-ball imaging. We compare our results with the well-known general fractional anisotropy (GFA) index using a fiber phantom comprising challenging diffusion profiles such as crossing, fanning and kissing fiber configurations and a human brain dataset considering the centrum semiovale. Additionally, we visualize the results directly on the fibers represented by streamtubes using a heat color map.

Keywords: Diffusion Tensor Imaging (DTI), Fiber Tractography, High Angular Resolution Diffusion Imaging (HARDI)

1. INTRODUCTION

Diffusion tensor imaging (DTI) is a method which measures the diffusion of water molecules. In fibrous tissue such as muscles or brain white matter the movement of water molecules is restricted, resulting in anisotropic diffusion. Based on the local diffusion profile, it allows for the identification of neuronal pathways and the approximation of the course of fibers in vivo. However, DTI is limited in terms of identifying multiple diffusion maxima within one voxel, caused by the Gaussian assumption of the tensor model. To overcome the limitations of DTI, high angular resolution diffusion imaging (HARDI) was introduced. HARDI techniques such as Q-ball imaging are able to resolve more than one diffusion orientation within one voxel. Hence, the differentiation between challenging intra-voxel fiber configurations such as fiber crossings, kissings or fannings and single fiber configurations is feasible. This information is especially needed in tractography approaches to guide the reconstruction of fiber pathways. For example, if challenging intra-voxel diffusion profiles are present, different heuristics are applied to determine the next step than in voxels containing single diffusion maxima. In neurosurgery, knowledge about the integrity of neuronal pathways is essential for pre-operative planning. Hence, it is important to differentiate diffusion profiles into the following three classes: voxels containing isotropic diffusion profiles, characterizing gray matter regions and voxels containing single or multiple fiber orientations, which are white matter regions.

However, existing diffusion classifiers are oftentimes not able to distinguish between gray and white matter and especially in white matter differentiate complex fiber distributions properly. In addition, classifiers are often of complex nature, not intuitive and easy to adjust for clinicians, since they need a detailed understanding of acquisition or reconstruction parameters. Therefore, in this paper we present an isotropic, single and multiple fiber classification index (ISMI) based on characteristics of the orientation distribution function (ODF), the local probability density function (PDF) describing the probability of a water molecule diffusing into a specific spatial

direction. We enable the classification of the diffusion profiles which is beneficial in tractography approaches to improve propagation as well as in neurological questions and neurosurgical planning concerning integrity and local fiber distributions. Furthermore, since we provide direct visual feedback within the proposed classification pipeline, the usability of our approach is very intuitive and easy to handle by clinicians.

2. RELATED WORK

In the following, a short literature study is presented, which aims to provide an overview on existing diffusion classifiers. In general, diffusion classification indices can be categorized into DTI- or HARDI-based, whereas in the latter case classifiers which aim to differentiate linear and more complex distributions, such as the ISMI, exist.

To rate the degree of linear diffusion of a distribution function within a voxel in DTI, the fractional anisotropy (FA)[1] is a well-known index, describing the degree of linearity of a diffusion distribution and is defined as follows:

$$FA = \sqrt{\frac{3}{2}} \frac{\sqrt{(\lambda_1 - \hat{\lambda})^2 + (\lambda_2 - \hat{\lambda})^2 + (\lambda_3 - \hat{\lambda})^2}}{\sqrt{\lambda_1^2 + \lambda_2^2 + \lambda_3^2}}, \tag{1}$$

where λ are the tensor eigenvalues and $\hat{\lambda}$ is the trace of the diffusion tensor. The generalized fractional anisotropy (GFA), introduced by Tuch,[2] is the adaption of the FA index to HARDI,

$$GFA = \frac{std(\Psi)}{rms(\Psi)} = \sqrt{\frac{n \sum_{i=1}^{n} \left(\Psi\left(\mathbf{u}_i\right) - \langle\Psi\rangle\right)^2}{(n-1) \sum_{i=1}^{n} \Psi\left(\mathbf{u}_i\right)^2}}. \tag{2}$$

Here, $\Psi(\mathbf{u})$ is the ODF value for a diffusion direction of interest $\mathbf{u}$, $\langle\Psi\rangle$ is the mean of the ODF and n is the number of samplings on a sphere, used to evaluate the ODF. A well-defined and rotationally invariant version of the GFA was defined by Landgraf et al.[3]

Since HARDI arose in diffusion imaging, indices aiming to delineate the true intra-voxel fiber population were developed. Frank et al.[4] introduced the fractional multifiber index (FMI) for determining the best describing model order, l, of the current diffusion probability function. The authors use spherical harmonic (SH) basis functions, to map the diffusion signal and determine the degree of complexity by analyzing the spherical harmonics coefficients of the current ODF,

$$FMI = \frac{\sum_{j:l\geq 4} |c_j|^2}{\sum_{j:l\geq 2} |c_j|^2} \tag{3}$$

where, c are the SH coefficients for order l. Chen et al.[5] and Descoteaux et al.[6] both introduced a similar diffusion index based on SH coefficients as well. The introduced indices are defined by

$$R_0 = \frac{|c_0|}{\sum_j |c_j|}, R_2 = \frac{\sum_{j:l=2} |c_j|}{\sum_j |c_j|}, R_{multi} = \frac{\sum_{j:l\geq 4} |c_j|}{\sum_j |c_j|}. \tag{4}$$

The underlying diffusion profile is considered to be isotropic if R_0 is large. However, if R_2 is large, a one-fiber distribution is present in the current voxel, whereas a large R_{multi}-value indicates more diffusion directions. We previously introduced an index called Morphological Fiber Classification (MFC)[7] which is not affected directly by acquisition parameters. The classifier detects multiple diffusion fiber directions using a white matter mask, resulting from ODF analysis. Within a global approach, the white matter mask is morphologically thinned out in a way that only clusters remain. Therefore, the classifier is only dependent on a proper white matter mask. These clusters occur at regions with complex morphology and are considered to represent voxels containing multiple diffusion orientations.

Despite the MFC, the presented classifiers lead to insufficient results in differentiating isotropic from anisotropic diffusion and in terms of anisotropic diffusion in single and multiple fiber orientation when using datasets with a low b-value and less diffusion gradient directions. Therefore, we developed ISMI, which consists of a classification pipeline and comprises a detailed analysis of the local diffusion distribution function.

3. METHODS

In the following, material and methods for ISMI computation and visualization will be introduced.

3.1 HARDI Datasets

Phantom We evaluated our classifier using a phantom dataset.[8–10] This phantom was originally provided by the Laboratoire de Neuroimagerie Assistée par Ordinateur (LNAO, France) in the course of the Fiber Cup, a tractography contest at the MICCAI conference in 2009. Data was acquired with two repetitions and 64 image encoding gradients. We averaged the two repetitions for further processing. The size was 64×64 voxels with a uniform voxel size of 3 mm and a b-value of 2000 s/mm^2.

Human Brain Furthermore, we applied ISMI to a human brain dataset of size $128 \times 128 \times 60$, acquired with a voxel size of $1.875 \times 1.875 \times 2$ mm.[11] The applied gradient direction scheme included 200 directions and a b-value of 3000 s/mm^2.

3.2 Reconstruction

Popular HARDI reconstruction methods are, amongst others, diffusion spectrum imaging (DSI),[12] spherical deconvolution (SD)[13] and Q-ball imaging.[2] DSI requires particular acquisition parameters (whole-sphere sampling), which leads to a detailed diffusion signal on the one hand, but on the other hand is, due to the acquisition time, not applicable in clinical routine examinations. SD is a HARDI-technique including previous knowledge about the underlying diffusion signal and therefore leads to sharper diffusion distributions. However, its susceptibility to noise leads to false positives and the integration of a single basic model, restricting the underlying diffusion shape, is problematic, since information is potentially lost. Q-ball imaging uses a single-sell acquisition scheme, which results in a shorter acquisition time. Furthermore, it does not make severe assumptions concerning the underlying diffusion profile as in SD and therefore, provides an appropriate balance for HARDI reconstruction and was chosen as the basis for our classifier. In the following, the implemented HARDI reconstruction using Q-ball imaging will be introduced.

Spherical harmonics form a complete orthogonal system, so an arbitrary real function $\Psi(\theta, \phi)$ can be expanded to comply spherical harmonics

$$\Psi(\theta, \phi) = \sum_{l=0}^{l_{max}} \sum_{m=-l}^{l} a_l^m Y_l^m(\theta, \phi), \tag{5}$$

where $Y_l^m(\theta, \phi)$ represents a spherical harmonic of order l and phase factor m. Further, a_l^m denotes the SH coefficient and l_{max} the truncation order of the spherical harmonics series. An analytical scheme to calculate appropriate SH coefficients for diffusion signal fitting was introduced by Descoteaux et al.[14] The authors additionally included a Laplace-Beltrami regularization term. They used a modified symmetric, real and orthonormal SH basis Y with elements Y_j as

$$Y_j = \begin{cases} \sqrt{2} \cdot \mathrm{Re}(Y_k^m), & \text{if } -k \leq m < 0, \\ Y_k^0, & \text{if } m = 0, and \\ \sqrt{2} \cdot \mathrm{Img}(Y_k^m), & \text{if } 0 < m \leq k, \end{cases} \tag{6}$$

where $Re(Y_k^m)$ and $Img(Y_k^m)$ denote the real and imaginary parts of Y_l^m and index $j = j(k, m) = \left(k^2 + k + 2\right)/2 + m$ and $k = 0, 2, 4, \ldots, l$ and $m = -k, \ldots, 0, \ldots, k$. Reformulating Equation 5 according to Equation 6 results in

$$\Psi(\theta_i, \phi_i) = \sum_{j=1}^{R} c_j Y_j(\theta_i, \phi_i), \tag{7}$$

for N gradient direction pairs θ_i, ϕ_i with $R = (l_{max} + 1)(l_{max} + 2)/2$ is the number of terms in the modifies SH basis. The proposed diffusion signal mapping for a chosen maximal model order results in a number of SH coefficients assigned to each term in the introduced modified SH basis, Equation 6.

4. DIFFUSION CLASSIFICATION

With previously defined HARDI reconstruction, evaluating the ODF is now simply solving Equation 7 for arbitrary diffusion directions of interest using the computed coefficients and corresponding basis functions. We evaluated the ODF for each voxel using a tessellation order 3 for a sphere. This results in 162 points, uniformly distributed over a sphere.

ISMI computation is illustrated schematically in Figure 1 and includes two major steps: first, the classification of white and gray matter and, secondly, the classification into single or multiple fiber populations. For the first step, we define a fiber mask identifying all voxels including white matter. Both, single and multiple fiber distributions belong to the same classification group. To differentiate between white and gray matter, the scaled sum of the min-max normalized ODF is calculated: We compute the ratio between the spherical function and the sphere, which is given by the maximal radius of the local ODF. Therefore, the white matter mask is defined by

$$1 - \frac{\sum_{i=1}^{n} \Psi\left(\mathbf{u}_i\right)}{n \cdot maxRad}, \tag{8}$$

where n is the number of samples on a sphere resulting from the icosahedron tessellation order and $\Psi\left(u\right)$ is the local ODF with diffusion directions of interest $\mathbf{u} = (\theta, \phi)$ with $\theta \in [0, \pi], \phi \in [0, 2\pi]$. The maximum radius of the current ODF is indicated by $maxRad$.

The next step aims to differentiate between single and multiple intra-voxel fiber distributions and is considered in the following only for voxels already classified to belong to white matter. Therefore, we can successfully classify between isotropic diffusion and multiple fiber orientations. To identify multiple diffusion directions, we compute the number of local maxima of the min-max normalized ODF above a certain threshold. For the phantom dataset, we chose a value of 0.5 and for the human brain 0.6. However, within the ISMI computation pipeline, the user can adjust the parameter with immediate visual feedback to control the impact of this classification stage and adjust the threshold for each diffusion dataset.

In a last step, we combine both classification results to form the ISMI, which finally differentiates between isotropic, single and multiple fiber configurations, as shown in Figure 1.

5. VISUALIZATION

This section aims to present the visualization of the ISMI index. We choose to enable a tract-specific visualization using a heat color map and texturing within a shader approach.

5.1 Color Map

To indicate the three different compartments, isotropic diffusion and single and multiple fiber distribution, we use a heat colormap. As visualized in Figures 2b, 3 and 4, isotropic diffusion profiles are indicated by white, single fiber distributions by yellow and more complex fiber configurations by red.

5.2 Fiber Tracts

To visualize the index with an anatomical and clinical meaning, we applied texture mapping to GPU-generated streamtubes. For tract generation, we used our distance-based HARDI tractography algorithm proposed in.[15] The deterministic approach bases on the local ODF and includes an evaluation of diffusion distributions in the seed voxel evaluation of distances to white matter boundaries in which vectors orthogonal to the current orientation are generated. In the proposed algorithm, curvature thresholds, local anisotropy information and the position of the current tract within the bundle are used to determine the direction for the next step in each voxel using the ODF.

The presented streamtubes are computed using a geometry shader-based pipeline, in which view vector oriented triangle strips are generated and tube-like colored in the fragment shader. More precisely, the distance of a fragment to the tube centerline is transferred from the geometry shader to the fragment shader and used to fade the fragment's color to black. Hence, a tube-like appearance is achieved without the computational

complexity of real tubes. The ISMI classification volume is an input for the shader pipeline and used in the fragment shader through texture lookup. In case the fragment is not faded to black, the previous color mapping is applied.

6. RESULTS

To evaluate the ISMI classifier, we compared our results with a well-known diffusion index, the GFA, introduced in Section 2. To identify challenging regions, and evaluate our method, we applied a tractography approach to the Fiber Cup phantom dataset, which comprises very challenging diffusion profiles such as crossing, kissing and fanning fiber configurations. Figure 2a shows the result using the GFA anisotropy index. Yellow indicates a high GFA-value and hence, high anisotropy, whereas red reveals isotropic regions with a low GFA-value. Using this index, regions with complex intra-voxel diffusion profiles such as crossings and fannings lead to a low anisotropy value. Considering regions where trajectories leak into gray matter, as one can see in Figure 2a in the left of the crossing at the bottom, leakings are not differentiated from crossings. As a consequence, GFA is not able to distinguish between regions with isotropic diffusion (gray matter) and multiple diffusion orientations (white matter). On the other hand, the ISMI classification results of the same fiber representation is shown in Figure 2b. The presented index successfully classifies into the three intra-voxel configurations: isotropic diffusion (white) single fiber population (yellow) and multiple fiber population (red). In crossing and fanning areas ISMI has a high value indicating multiple fiber configurations, whereas the leaking of the trajectory leads to a low value. If we compare both results, we can see that GFA indicates false-positives in terms of multiple fiber orientations, such as leakings of the fiberpathway into gray matter or in regions with high curvature. Contrary, ISMI is able to differentiate between isotropic diffusion and multiple fiber populations.

Figure 3 shows fibers belonging to the corpus callosum and running in the centrum semiovale, a region in the brain where fibers of the corticospinal tract, the superior longitudinal fasciculus and the corpus callosum meet. For better spatial orientation, the anatomical volume is visualized as well. This leads to challenging crossing configurations of all three tracts within voxels. In addition, the corpus callosum fans into the whole hemisphere, which cannot be reconstructed using simple tractography approaches. The parts of the reconstructed callosal fibers, crossed by other neuronal pathways, can be identified in Figure 3, since they are colored in red: In the right and the left part of the illustrated fibers, red parts belong to the centrum semiovale. However, red parts in the center of the corpus callosum reveal regions where the cingulum and the corpus callosum meet. The cingulum is a pathway running on top of the corpus callosum in the opposite direction.

In order to illustrate the classification power in terms of isotropic diffusion, Figure 4 shows parts of the corpus callosum but reconstructed with a tractography approach which only takes the maximum value of the ODF as a tracking direction. Hence, this simple algorithm is not able to reconstruct challenging fiber configurations properly, the fanning of the corpus callosum in this case. Additionally, a seed region within gray matter was placed to indicate false positives, as can be seen below the center of the corpus callosum. Fibers in this region are displayed in white. We can observe that fibers running inferiorly are white as well and thus isotropic. These parts of the reconstructed neuronal pathways therefore run into gray matter areas or show a very low anisotropy, which corresponds with knowledge about diffusion imaging in fibers close to the head's surface.

7. DISCUSSION AND CONCLUSION

The novelty of the presented work consists of the ISMI index which successfully classifies diffusion into the following three compartments: isotropic diffusion profiles and anisotropic diffusion into single and multiple fiber populations. Contrary to known classifiers, such as the GFA, the presented index additionally provides the ability to control the extent of multiple fiber configurations by adjusting the threshold for the number of maxima of the ODF. Therefore, the user can directly determine and explore challenging fiber configurations of interest with a visual feedback. The introduced computation pipeline and the immediate visual feedback facilitates an intuitive handling and control of the classification result. In addition, a following fiber integrity examination considering only single fiber distributions is feasible. To our knowledge, no index based on Q-ball imaging revealing this detailed information about the true underlying diffusion profile exists.

For this work Q-ball imaging was chosen as a reconstruction method. However, any HARDI-technique, resulting in an ODF, can act as an input for our classifier.

The presented index ISMI proved to be beneficial in terms of the intra-voxel diffusion classification problem. It is able to identify isotropic diffusion from multiple orientations within one voxel. Therefore, tractography approaches or fiber integrity examinations can be improved for neurological examinations or neurosurgical planning.

REFERENCES

[1] Basser, P. J. and Pierpaoli, C., "Microstructural features measured using diffusion tensor imaging," *Journal of Magnetic Resonance* , 209–219 (1996).

[2] Tuch, D. S., "Q-ball imaging," *Magnetic Resonance in Medicine* **52**(6), 1358–1372 (2004).

[3] Landgraf, P., Merhof, D., and Richter, M., "Anisotropy of HARDI diffusion profiles based on the L2-Norm," *Proc. Bildverarbeitung für die Medizin* , 239–243 (2011).

[4] Frank, L. R., "Characterization of anisotropy in high angular resolution diffusion-weighted MRI," *Magnetic Resonance in Medicine* **47**, 1083–1099 (2002).

[5] Chen, Y., Guo, W., Zeng, Q., Yan, X., Huang, F., Zhang, H., He, G., Vemuri, B. C., and Liu, Y., "Estimation, smoothing, and characterization of apparent diffusion coefficient profiles from high angular resolution DWI," *Computer Vision and Pattern Recognition* **1**, 588–593 (2004).

[6] Descoteaux, M., Angelino, E., Fitzgibbons, S., and Deriche, R., "Apparent diffusion coefficients from high angular resolution diffusion images: Estimation and applications," *Magnetic Resonance in Medicine* **56**, 395–410 (2006).

[7] Röttger, D., Seib, V., and Müller, S., "MFC: A morphological fiber classification approach," *Proc. Bildverarbeitung für die Medizin* (2011).

[8] Poupon, C., Rieul, B., Kezele, I., Perrin, M., Poupon, F., and J.F., M., "New diffusion phantoms dedicated to the study and validation of HARDI models," *Magnetic Resonance in Medicine* **60**(6), 1276–83 (2008).

[9] Fillard, P., Descoteaux, M., Goh, A., Gouttard, S., Jeurissen, B., Malcolm, J., Ramirez-Manzanares, A., Reisert, M., Sakaie, K., Tensaouti, F., Yo, T., Mangin, J.-F., and Poupon, C., "Quantitative evaluation of 10 tractography algorithms on a realistic diffusion MR phantom," *NeuroImage* (In press).

[10] Poupon, C., Laribire, L., Tournier, G., Bernard, J., Fournier, D., Fillard, P., Descoteaux, M., and Mangin, J.-F., "A diffusion hardware phantom looking like a coronal brain slice.," *Proc. ISMRM* (2010).

[11] Poupon, C., Poupon, F., Allirol, L., and Mangin, J.-F., "A database dedicated to anatomo-functional study of human brain connectivity," *Proc. 12th HBM Neuroimage* (646) (2006).

[12] Wedeen, V. J., Reese, T. G., Tuch, D. S., Weigel, M. R., Dou, J., Weiskoff, R. M., and Chessler, D., "Mapping fiber orientation spectra in cerebral white matter with fourier-transform diffusion MRI," *Proc. of the International Society of Magnetic Resonance in Medicine* **8**, 82 (2000).

[13] Tournier, J.-D., Calamante, F., Gadian, D. G., and Connelly, A., "Direct estimation of the fiber orientation density function from diffusion-weighted MRI data using spherical deconvolution," *NeuroImage* **23** (2004).

[14] Descoteaux, M., Angelino, E., Fitzgibbons, S., and Deriche, R., "Regularized, fast and robust analytical Q-ball imaging," *Magnetic Resonance in Medicine* **58**, 497–510 (2007).

[15] Röttger, D., Seib, V., and Müller, S., "Distance-based tractography in high angular resolution diffusion imaging," *The Visual Computer* **27**, 729–739 (2011).

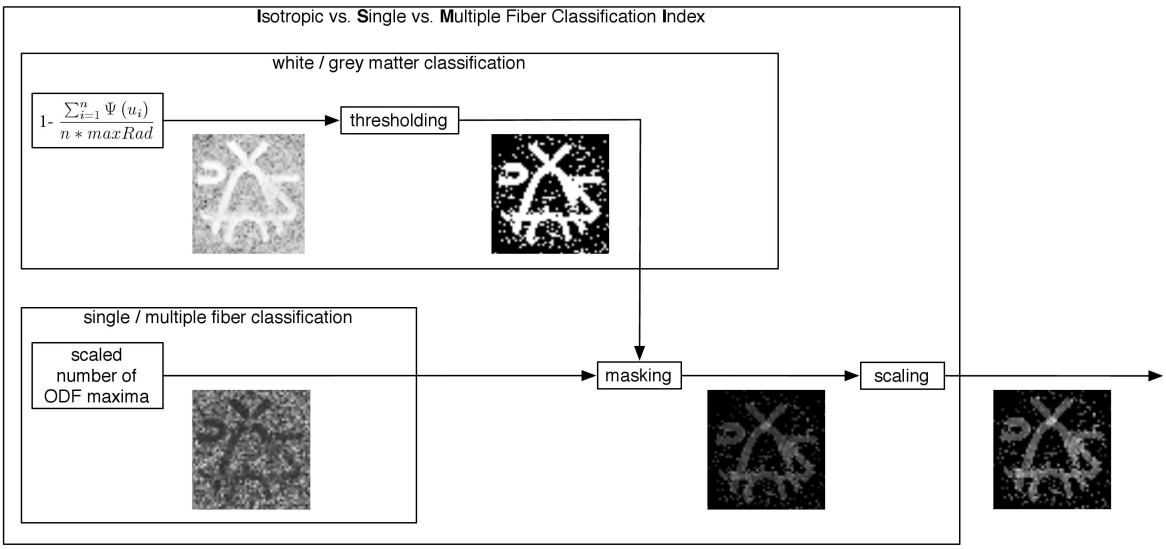

Figure 1: Computation pipeline for ISMI calculation using a phantom dataset.

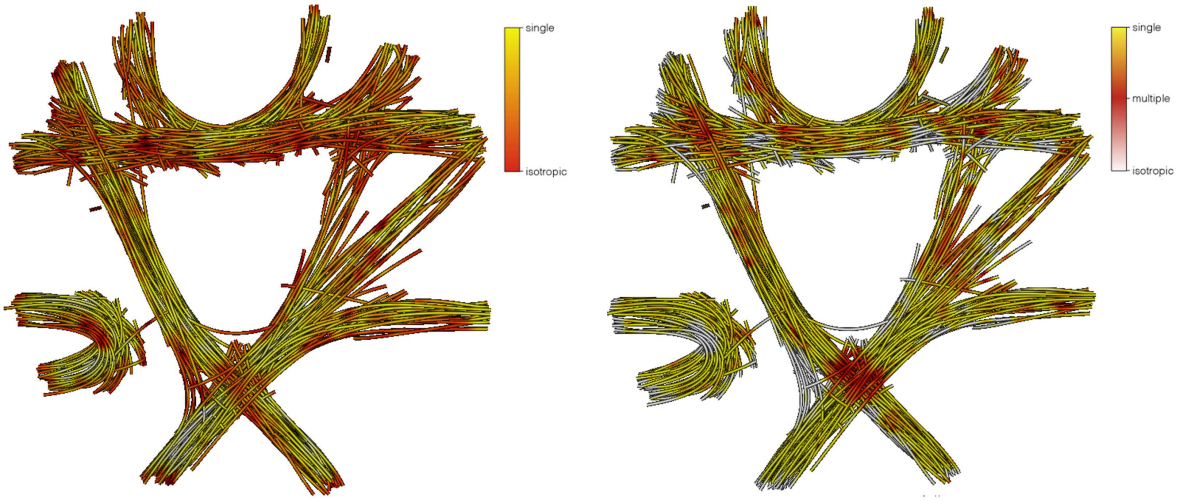

(a) (b)

Figure 2: (2a) Visualization of GFA index results. Red parts indicate regions with low anisotropy, yellow parts indicate high anisotropy. Evidently, using GFA is not an option for clear differentiations between multiple fiber populations and isotropic regions, both result in similar color values. (2b) Classification results of ISMI. Accurate classification of isotropic diffusion (white), single fiber (yellow) and multiple fiber distribution (red) is achieved.

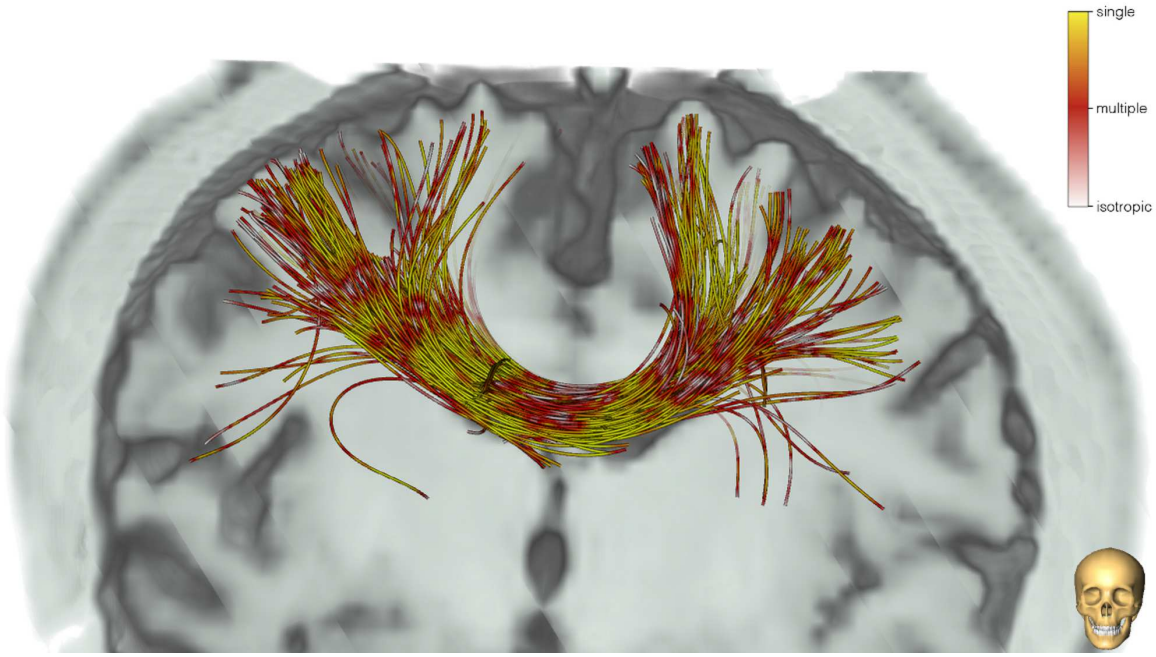

Figure 3: ISMI classification results for callosal fibers of a human brain, visualized with an anatomical volume.

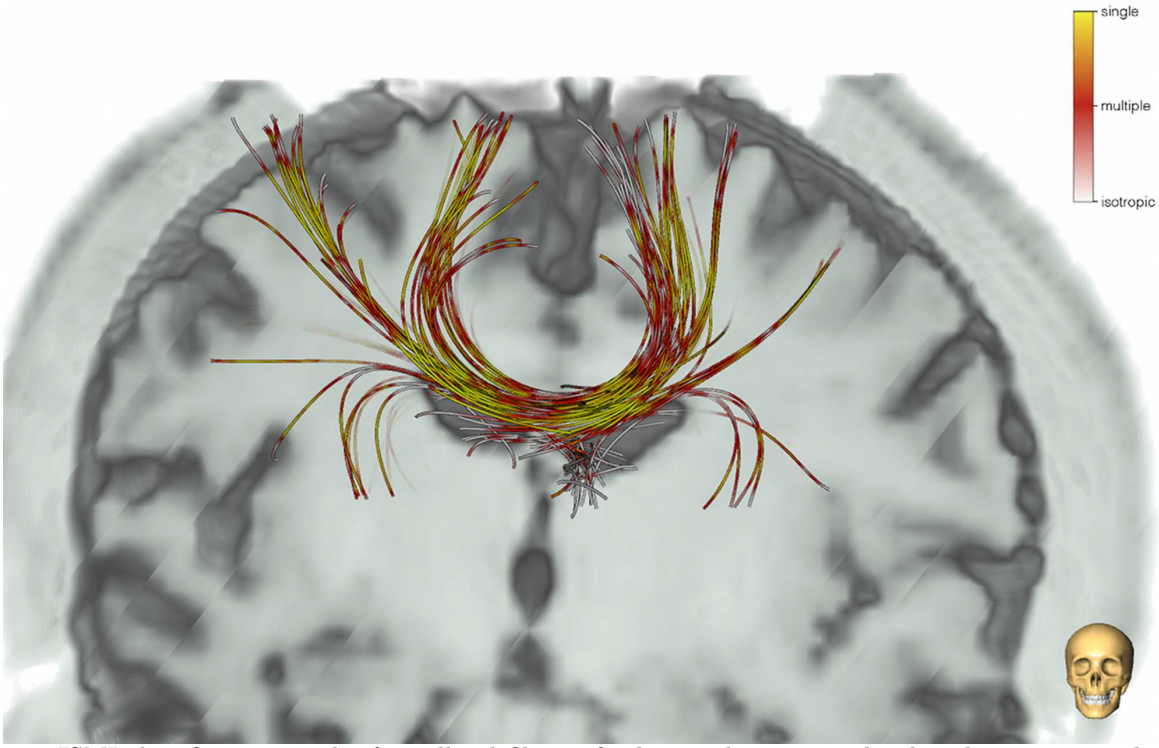

Figure 4: ISMI classification results for callosal fibers of a human brain, visualized with an antomical volume and tractography results using a simple tracking algorithm.